

Discovering transiting exoplanets

LAB COURSE - MODERN PHYSICS

HS2024

Authors:

Brice-Olivier Demory

Last update: September 22, 2025

u^b

Contents

Introduction	2
1 Introduction	2
1.1 Description of the transit method	2
1.1.1 Transit geometry	2
1.1.2 Measured parameters	2
1.1.3 Uncertainties	4
1.2 Other applications	5
1.2.1 Occultation and thermal emission	5
1.2.2 Transmission spectroscopy	6
2 Facilities	6
2.1 SAINT-Ex Observatory	6
2.2 TESS	7
3 Software and further information	8
4 Methodology	8
4.1 Candidate identification	8
4.2 Observing strategy and planning	8
4.3 Data reduction	9
4.4 Data analysis	9
4.5 Data formatting	9
References	10
A File formatting with AIJ	11

1 Introduction

The scope of this experiment is to obtain transit data of new small exoplanets using the NASA TESS space mission and the Saint-Ex ground-based observatory. The data obtained in the frame of this practical work might be used in peer-reviewed publications in the future (where your contribution will be acknowledged), hence the importance of being rigorous at all stages and carefully document the work.

In a nutshell, the proposed work involves the identification of a compelling target from the TESS archive, the observation planning with the Saint-Ex telescope, the execution of these observations, the reduction and analysis of the data, the formatting of the data for sharing with other astronomers.

1.1 Description of the transit method

The transit method has been extremely prolific since the beginning of the 2000s. In particular, it allows the direct determination of the ratio of the radius of the planet to the radius of the star, the stellar density and the orbital period, from the measurement of the flux drop induced by the planet crossing the stellar disc. Combined with Doppler spectroscopy, the transits allow the mass to be determined thanks to knowledge of the inclination, which would be otherwise degenerate. By obtaining the radii and masses of planets, we can compare our theoretical understanding of the bulk structure of these objects with observations.

1.1.1 Transit geometry

The geometry used to observe the passage of a planet in front of its star is highly constrained. Thus, assuming zero eccentricity, the probability of observing a transit is given by $\frac{R_\star + R_P}{a}$. Short-period planets orbiting a large star are therefore favoured. This amounts to a constraint on the orbital inclination of the planet i such that $a \cos i \leq R_\star + R_P$. In our solar system, this gives a transit probability for Mercure of 1.2% at around 0.4 AU, compared with only 0.07% for Saturn at 10 AU. This observation motivates, on the one hand, the continuous observation of several hundred stars (as done by space-borne surveys (CoRoT, Kepler, TESS...)) and, on the other hand, a selection of the planets with the shortest orbital periods discovered by radial velocities. Indeed, if we consider the first discovered extrasolar planet, 51 Peg b [1], its transit probability exceeds 10% and occur every 4 days. The large number of hot Jupiters discovered so far suggests that the prospects for this approach are bright. Finally, the simplicity with which this method can be implemented means that even people with a small telescope can participate in the monitoring of known planets or search for transits of already-discovered Jupiter planets by radial velocities around bright stars.

Figure 1 shows the geometry of a transit, where the orbital inclination of the planet is close to perfect alignment with the observer's line of sight. Figure 2 shows a transit light curve measured by the Hubble Space Telescope (HST) with a very high signal-to-noise ratio.

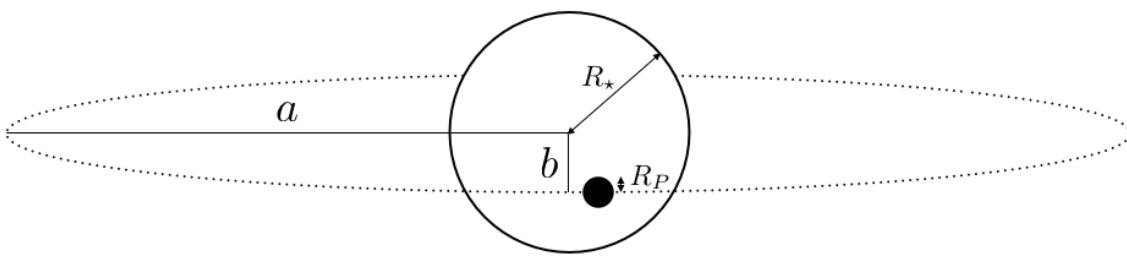


Figure 1: **Transit geometry.** The scale is arbitrary but remains similar to some hot-Jupiter systems that have already been discovered. a represents the orbital semi-major axis, b the impact parameter, with $b = a \cos i$. R_P et R_\star representing the planetary and stellar radii, respectively.

1.1.2 Measured parameters

Figure 3 shows schematically the different phases of a planet transit with a sketch of the flux variation during the event. Note the influence of the impact parameter b , which can significantly affect the light curve's duration. The light curve measurement makes it possible to determine the depth and duration of the transit, the impact parameter giving the shape of the transit and the stellar density, as shown below:

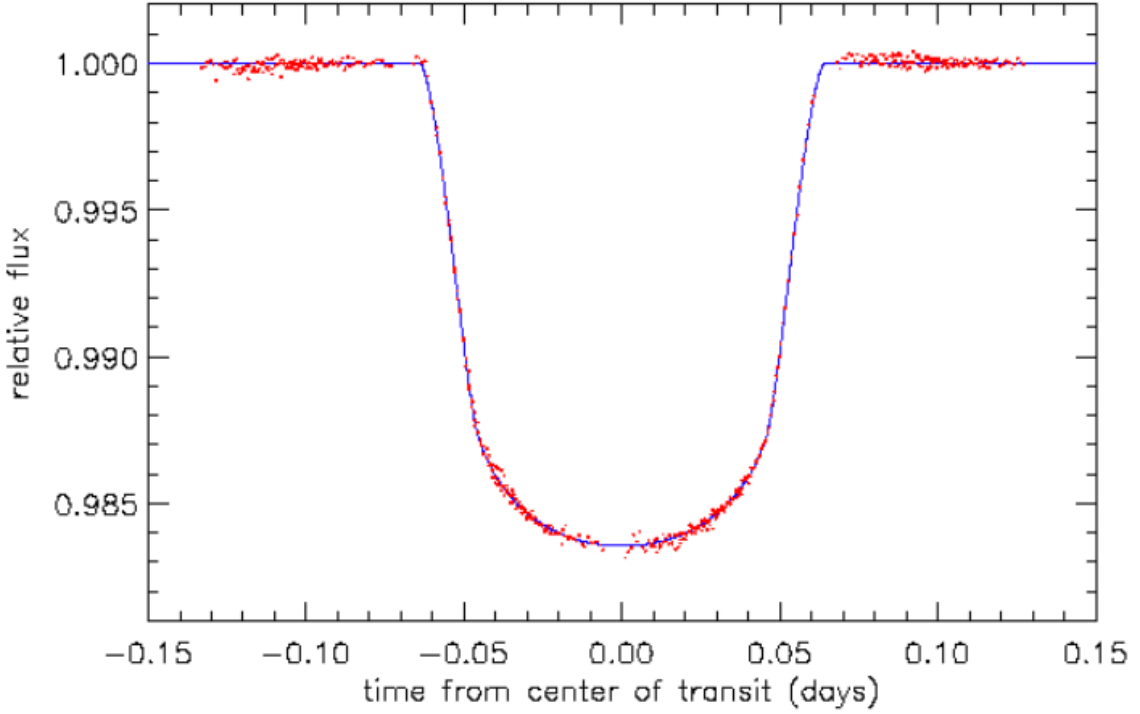


Figure 2: HD 209458 b transit light curve obtained by HST [2].

Transit depth The transit depth informs about the maximum fraction of the stellar disk blocked by the planet. In our case, we neglect the effects of limb-darkening.

$$\frac{\Delta F}{F_0} = \frac{R_P^2}{R_\star^2} \quad (1)$$

In the case of a Jupiter orbiting a solar-type star, the drop in flux is around 1%, whereas for the favourable situation of an Earth orbiting a typical M dwarf, the corresponding drop in flux will be of the order of 0.1%.

Transit duration The total transit duration (between 1st and 4th contacts) for a circular orbit can be calculated as follows:

$$T_{14} = \frac{PR_\star}{\pi a} \sqrt{\left(1 + \frac{R_P}{R_\star}\right)^2 - \left(\frac{a}{R_\star} \cos i\right)^2} \quad (2)$$

where P is the planet's orbital period.

Impact parameter This parameter corresponds to the determination of the inclination of the system, and is calculated as follows [3]:

$$b = \frac{a}{R_\star} \cos i \quad (3)$$

$$= \sqrt{\frac{(1 - \sqrt{\Delta F})^2 - (1 + \sqrt{\Delta F})^2 \frac{\sin^2(\pi T_{23}/P)}{\sin^2(\pi T_{14}/P)}}{1 - \frac{\sin^2(\pi T_{23}/P)}{\sin^2(\pi T_{14}/P)}}} \quad (4)$$

By determining i , we can obtain the exact mass of the planet from $M_P \sin i$ obtained by radial velocities.

Stellar density It is also possible to obtain stellar density from a transit curve and Kepler's 3rd law. Kepler's 3rd Law gives us the mass located within the orbit of the planet, and the radius of the star is constrained by the transit duration (cf. eq. 2) [3].

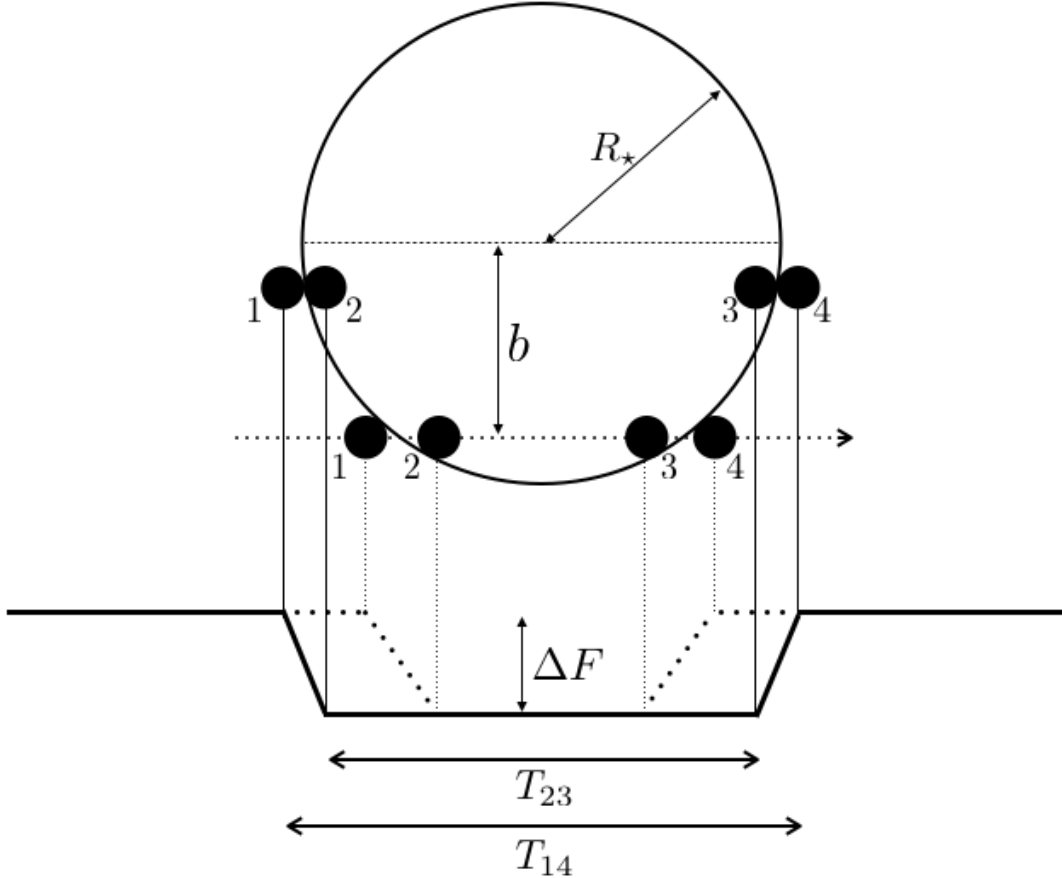


Figure 3: Sequence of the transits with the associated simplified light curve. Contacts 1 to 4 are shown for two different impact parameters, as well as the resulting light curve. The various observables used to define the derived parameters are shown in the figure.

$$\rho_{\star} = \frac{4\pi^2}{GP^2} \left(\frac{(1 + \sqrt{\Delta F})^2 - b^2(1 - \sin^2(\pi T_{14}/P))}{\sin^2(\pi T_{14}/P)} \right)^{\frac{3}{2}} \quad (5)$$

Obtaining the stellar radius as such requires the use of a mass-radius relationship for a specific stellar spectral type (see below).

1.1.3 Uncertainties

We will not discuss the astrophysical sources that can mimic a planetary transit (grazing binary, M-dwarf transit whose radius is compatible with a planet, spots, binary with background clipping, etc.), but we will mention a few sources of uncertainty that can affect the model fit:

Eccentricity Eccentricity plays an important role in the determination of most of the parameters described above. The concern for simplicity which has led us not to include it in the equations should not obscure the effects of its non-inclusion. Most transit planets have short orbital periods. It is therefore usual to invoke in these cases the small circularisation time[4] :

$$t_{circ} = \frac{4}{63} Q_P \frac{P}{2\pi} \frac{M_P}{M_{\star}} \left(\frac{a}{R_P} \right)^5 \quad (6)$$

to assume a circular orbit ($e = 0$). For instance, [5] show the dependence of the stellar density with orbital eccentricity e and the argument of periastron ω .

This constraint is justified by the fact that the radial velocities published by [6] are compatible with a circular orbit. However, even a small e can impact $e \sin \omega$ and $e \cos \omega$, without being notably constrained by radial velocities.

The origin of this error can most certainly be traced back to the comparison of the time taken to circulate the planetary orbit with the age of the star $t_{circ} \ll age_\star$. Wrong assumptions about the system [7] and an ill-defined Q factor not excluding a marginally non-null eccentricity.

Limb-darkening The bottom of the transit curves is generally not flat for observations made in the visible. This effect, attributed to limb-darkening, is due to the fact that the light intensity coming from the telescope is not constant across the disc and is at its maximum at the centre of the disc. Figure 4 illustrates the influence of this parameter.

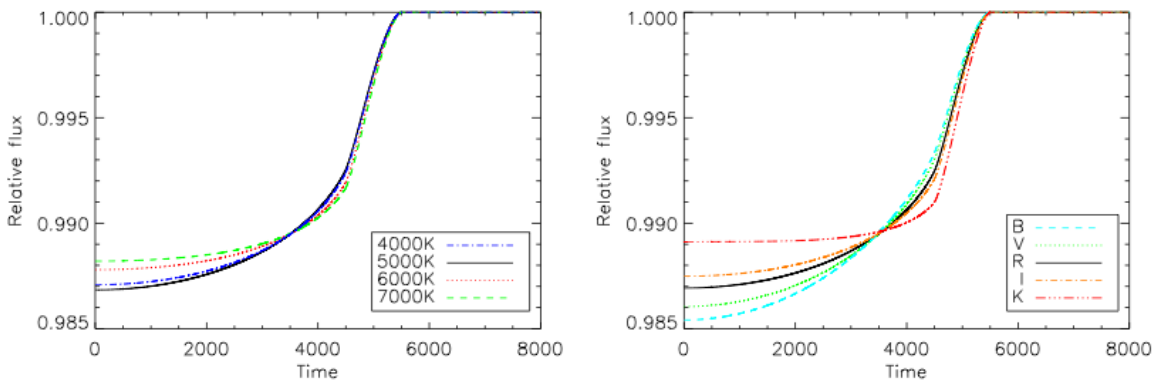


Figure 4: Limb-darkening incidence on transit light curves. Modelling a Saturn transit for different stellar temperatures (left) and for observation in different filters (right). Credit : [8]

The advantage of observing in the near infrared is obvious, since the corresponding K-band model shows a background that is significantly flatter than in the visible.

Stellar radius The combination of photometry and spectroscopic data does not make it possible to obtain the uniqueness of the radii and masses of the planet and the star [9]. Stellar evolution models must be employed and the stellar density ρ_\star as defined below must be taken into account as additional constraints. A global minimisation on $[Fe/H]$, T_{eff} and ρ_\star) has to be done from a grid of models calculated for the relevant isochrones. The interpolation in this parameter space yields estimates for the stellar radius and mass. The uncertainties of this approach can become prominent, particularly for low-mass stars, while one ideally wants to obtain a direct measurement of the diameter of an exoplanet host star using interferometry, for instance. Unfortunately this approach is possible only for the closest stars as more distant ones are too small.

1.2 Other applications

As we saw above, a transiting planet makes it possible to characterise its radius and mass. It is interesting to explore the other observation possibilities offered in this specific case. Figure 5 shows schematically the information on the physics of the atmosphere and the internal structure of the planet that can be deduced when its orbital plane coincides with the line of sight.

It should be noted that observing the orbital phase modulation does not necessarily imply that the planet needs to transit its star but could also have an inclined orbital plane with respect to the line of sight.

1.2.1 Occultation and thermal emission

Detecting the occultation of a planet is facilitated by the use of an infrared instrument to take advantage of the more favourable planet/shield contrast. Calculating the effective temperature of the planet is then easy if we assume that the depth of the occultation is the emissivity ratio of the two objects, which could be distorted by cloud layers that significantly modify the planetary albedo or the presence of an inversion layer in the upper atmosphere.

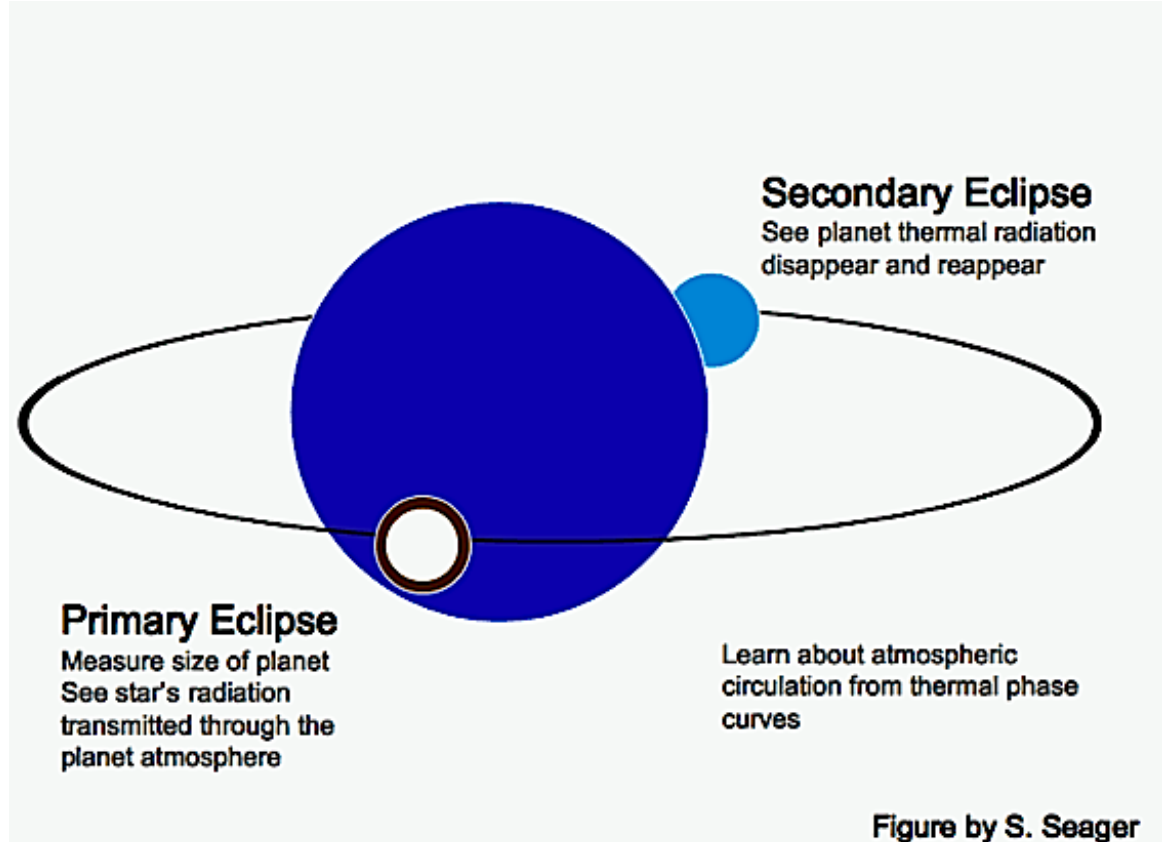


Figure by S. Seager

Figure 5: The primary eclipse is the transit and has already been discussed above. If the atmosphere scale-height is large enough, differential molecular absorption by the planet atmosphere could be detected by observing the transit at multiple wavelengths. The secondary eclipse (*occultation* is to be preferred), occurs when the planet passes behind its star and the planet's brightness temperature could be determined. Observing all along the orbit enables to capture the phase-dependent planet emission properties. Credit : S. Seager

1.2.2 Transmission spectroscopy

With sufficient spectral resolution, the depth of the transit depends on the wavelength as it becomes sensitive to absorption by the elements present in the planet's atmosphere. The first detection of an exoplanet atmosphere has been achieved on HD 209458 b, with the detection of Na using transmission spectroscopy [10]. Sodium had been theoretically predicted as a clear signature in hot gas giant atmospheres beforehand [11]. Using this same technique in the UV from space with HST, hydrogen (Ly α line) [12] as well as oxygen and carbon had been detected in the same exoplanet. Attempts to perform transmission spectroscopy on this object from the ground were unsuccessful, largely because of the Earth's atmosphere. The use of space-based means (HST) was necessary to obtain these results. The transit of HD 209458 b in Ly α is characterised by a depth of 15%, which led the authors to invoke ongoing escape of the planet's atmosphere.

2 Facilities

This section gives a brief description of the facilities that will be used in this experiment

2.1 SAINT-Ex Observatory

The SAINT-EX Observatory¹ (Search And characterisatioN of Transiting EXoplanets) has been commissioned in March 2019. SAINT-EX is a 1-m F/8 Ritchey-Chrétien telescope built by the ASTELCO company and uses a similar design to the telescopes of the SPECULOOS Southern Observatory [13, 14]. SAINT-EX is located at the Observatorio Astronómico Nacional, in the Sierra de San Pedro Martir in Baja California, México (31.04342 N, 115.45476 W) at 2780 m altitude. The telescope is installed on an ASTELCO equatorial NTM-1000 mount equipped with direct-drive motors, which enables operations without meridian flip. The telescope is installed

¹https://www.saintex.unibe.ch/saint_ex_observatory/

in a 6.25-m wide dome built by the Gambato company. In terms of mount performance, SAINT-EX typically achieves a RMS better than 3 arcsec relative to the pointing model and a tracking accuracy – without autoguiding – better than 2 arcsec over 15-min timescales. To improve this figure further, SAINT-EX uses the DONUTS autoguiding software [15], which increases the guiding precision to 0.2 arcsec RMS or better that is less than a pixel. SAINT-EX is equipped with an Andor iKon-L camera that integrates a deep-depletion e2v 2K × 2K CCD chip with a BEX2-DD coating that is optimised for the near infrared (NIR). The filter wheel includes the Sloan *ugriz'* broad-band filters, as well as special blue-blocking (transmittance > 90% beyond 500 nm) and NIR (transmittance > 95% beyond 705 nm) filters. The detector gives a field of view of 12 arcmin × 12 arcmin with 0.34 arcsec per pixel.

SAINT-EX operations are robotic and the data reduction and analysis are automated by a custom pipeline PRINCE (Photometric Reduction and In-depth Nightly Curve Exploration) that ingests the raw science and calibration frames and produces light curves using differential photometry. The PRINCE pipeline performs standard image reduction steps, applying bias, dark, and flat-field corrections. Astrometric calibration is conducted using Astrometry.net [16] to derive correct world coordinate system (WCS) information for each exposure. Photutils star detection [17] is run on a median image of the whole exposure stack to create a pool of candidate stars in the field of view. Stars whose peak value in the largest aperture is above the background by a certain threshold, defined by an empirical factor times the median background noise of the night, are kept as reference stars for the differential photometric analysis. From the WCS information and the detected stars' coordinates, the pipeline runs centroiding, aperture and annulus photometry on each detected star from the common pool, using LMFIT [18] and Astropy [19, 20], and repeats this for each exposure to obtain the measured lightcurves for a list of apertures. The measured lightcurves for each aperture are corrected for systematics using either a PCA approach [21] or a simple differential photometry approach that corrects a star's lightcurve by the median lightcurve of all stars in the pool except for the target star.

2.2 TESS²

The Transiting Exoplanet Survey Satellite (TESS) is a NASA astrophysics mission designed to conduct an extensive survey of exoplanets using the transit photometry method. Launched on April 18, 2018, TESS is a key component of NASA's Exoplanet Exploration Program, aimed at identifying and characterising exoplanets around bright, nearby stars.

TESS is equipped with four identical wide-field cameras, each featuring a 16.5deg × 24deg field of view, resulting in a total effective field of view of 24deg × 96deg. Each camera utilises a 4K × 4K CCD (Charge-Coupled Device) sensor with a pixel scale of 21 arcseconds per pixel, optimised for high-precision photometry in the visible to near-infrared spectrum (600-1000 nm). The optical design incorporates a custom broadband filter with a peak transmission of approximately 80% to maximise the signal-to-noise ratio (SNR) for stellar brightness measurements.

The cameras are mounted on a stable, thermally controlled platform to minimise thermal noise and ensure consistent performance. The optical system employs a fast f/1.4 aperture, which allows for a high throughput of light, critical for detecting the minute brightness variations associated with planetary transits.

TESS employs a two-year survey strategy, divided into 26 sectors, each covering an entire field of view. Each sector is observed for a continuous period of 27 days, followed by a 13-day data downlink period. The survey strategy is designed to maximise the number of transits observed for each target star, with a focus on stars brighter than magnitude 12, which are ideal for follow-up observations (e.g. with the James Webb Space Telescope). The satellite operates in a highly elliptical orbit with a period of approximately 13.7 days, allowing for continuous observation of each sector. The orbit is designed to minimise the effects of Earth's atmosphere and light pollution, enhancing the quality of the photometric data.

The data collected by TESS is processed using the TESS Science Processing Operations Center (SPOC), which employs advanced algorithms for data reduction. Key steps in the data processing pipeline include: 1) Preprocessing: Raw data is calibrated to remove instrumental effects, including pixel-to-pixel sensitivity variations and cosmic ray hits, 2) Light Curve Extraction: The calibrated data is used to generate light curves for each target star, employing aperture photometry techniques to optimise the extraction of stellar flux, 3) Systematic Noise Removal: Advanced techniques, such as Principal Component Analysis (PCA) and Gaussian Process Regression, are applied to mitigate systematic noise and improve the precision of the light curves, 4) Transit Detection: The processed light curves are analysed using the Box Least Squares (BLS) algorithm to identify periodic transit signals, allowing for the detection of exoplanet candidates.

²This subsection was generated with GPT4

3 Software and further information

It is recommended to have a look at the resources below before starting the experiment:

- An up-to-date list of TESS confirmed/validated exoplanets or candidates can be found here:
<https://exofop.ipac.caltech.edu/tess/>
- More details on astronomical and exoplanet observations, one could read this introductory document, by D. Conti (<https://astrodenni.com/Guide.pdf>).
- To facilitate the work and make it compatible with the lab timeframe, the data analysis (from reduced data to planet parameters) could be conducted with the AstroImageJ software (<https://www.astro.louisville.edu/software/astroimagej/>).

4 Methodology

Make sure to be familiar with the overall experiment, by going through the introduction section and references. In this section, we describe the different parts of the work that will have to be completed:

4.1 Candidate identification

The most important part of the experiment is to select a scientifically compelling target. Saint-Ex is optimised to perform observations of cool stars, so to leverage this advantage, focus your search on small host stars (M spectral type and latter), which are cooler and thus redder than their more massive siblings. In your report, motivate the target choice with an interesting science question. We do not observe a star or a planet randomly, but because we want to investigate something. It could be on Jupiter-sized exoplanets around the smallest stars (how frequent are they? Since they are rare these objects are particularly interesting), or on close-in rocky planets with orbital periods less than a day to study their surfaces or secondary atmospheres if any... This practical work could also be used to obtain the transit light curve of a candidate in another bandpass than TESS, to confirm achromaticity, thus that the candidate is a planet and not a false positive (e.g. background eclipsing binary).

The main resource for that part of the work is the Exoplanet Follow-up Observing Program (ExoFOP) website (see Section 3), which summarises all TESS planet candidates but also the observations obtained so far for each of them. A good starting point is the list of current TESS Objects of Interest (TOI), which summarises the key parameters of all candidates identified so far (some may be bona fide planets, some may be false positives). A direct link to this large table can be found here: https://exofop.ipac.caltech.edu/tess/view_toi.php. *Tip:* 1) look at the comments in the table, 2) make sure to download the whole table to your computer to facilitate ordering, edits, colouring, etc.

One possible check at this stage is to only down-select candidates that are bright enough to be observed for a given transit depth. For this, the Saint-Ex Exposure Time Calculator will be useful (<https://www.saintex.space/etc/king/ProgValeur.html>)

4.2 Observing strategy and planning

Once the target is identified, it is necessary to check that the planet candidate can be observed. The table contains both the orbital period and the epoch at which the transit occurs (in Julian day – JD). Then, we need to find out whether a given transit can actually be observed with Saint-Ex. First, identify the nights when the observations will have to take place. Since the actual work on the experiment is a few weeks only, plan for the upcoming nights. Based on the sky coordinates of the target in the TOI list, find out whether the host star is actually observable at this time of the year and whether the transit timespan can be observed in full during night time. Saint-Ex coordinates are the following: 31.043416667 North, -115.454763889 West, altitude is 2780m above mean sea level. Make sure to also include a minimum of 1h extra time before and after the transit itself to facilitate the data analysis.

It is critical to triple check the feasibility phase of the observations as these inputs will be directly submitted to the telescope observing queue. Using the inputs above, send the current information to the Teaching Assistant:

- Start time
- End time
- Target name

- Target right ascension (J2000 epoch)
- Target declination (J2000 epoch)
- Filter
- Exposure time (based on ETC estimates)

4.3 Data reduction

After the observations are completed, PRINCE will automatically reduce and process the data, typically during early evening (European time). A report will be produced showing whether the observations had been successful or not. Closely inspect the report at this stage. If the observations failed (weather, technical issue...), make sure to have a contingency plan (other target with a visible transit).

Once these checks are done, use AstrolImageJ (AIJ) to perform your own data reduction. First, make sure to adjust the software configuration and learn about the data reduction process using the documentation. Then load the raw frames in AIJ (science, bias, darks, flats) to generate calibrated images, which will complete the data reduction.

4.4 Data analysis

The data analysis starts from the calibrated images from the previous step and carries on until light curves are produced. This step entails plate solving (matching image spatial coordinates with sky coordinates), identify the target and suitable reference stars, perform differential photometry and fit the data. All these steps require multiple iterations to identify the optimal parameters (e.g. best aperture size yielding the smallest scatter, background annulus size, choice of reference stars...). The model fit is the very last step and will adjust a theoretical transit model to the data, to derive the planet physical parameters. Make sure to exploit all resources on the use of AIJ to fully exploit the data obtained with Saint-Ex.

4.5 Data formatting

A final step is to prepare the data so it can be shared with the wider community. This can be conveniently done within AIJ, with the correct plot parameters. The procedure is indicated in the Appendix (adapted from TFOP SG1 guidelines).

References

- [1] Mayor, M. & Queloz, D. A Jupiter-mass companion to a solar-type star. *Nat* **378**, 355–359 (1995).
- [2] Brown, T. M., Charbonneau, D., Gilliland, R. L., Noyes, R. W. & Burrows, A. Hubble space telescope time-series photometry of the transiting planet of hd 209458. *ApJ* **552**, 699 (2001).
- [3] Seager, S. & Mallén-Ornelas, G. A unique solution of planet and star parameters from an extrasolar planet transit light curve. *ApJ* **585**, 1038 (2003).
- [4] Rasio, F. A., Tout, C. A., Lubow, S. H. & Livio, M. Tidal decay of close planetary orbits. *Astrophysical Journal* v.470 **470**, 1187 (1996).
- [5] Winn, J. N. *et al.* The Transit Ingress and the Tilted Orbit of the Extraordinarily Eccentric Exoplanet HD 80606b. *ApJ* **703**, 2091–2100 (2009). [0907.5205](#).
- [6] Wilson, D. M. *et al.* Wasp-4b: A 12th magnitude transiting hot jupiter in the southern hemisphere. *ApJ* **675**, L113 (2008).
- [7] Jackson, B., Barnes, R. & Greenberg, R. Tidal heating of terrestrial extrasolar planets and implications for their habitability. *MNRAS* **391**, 237–245 (2008). [0808.2770](#).
- [8] Moutou, C. & Pont, F. Detection and characterization of extrasolar planets: the transit method. *Proceedings Goutelas* 25 (2006).
- [9] Torres, G., Winn, J. N. & Holman, M. J. Improved parameters for extrasolar transiting planets. *ApJ* **677**, 1324 (2008).
- [10] Charbonneau, D., Brown, T. M., Noyes, R. W. & Gilliland, R. L. Detection of an extrasolar planet atmosphere. *ApJ* **568**, 377 (2002).
- [11] Seager, S., Whitney, B. A. & Sasselov, D. D. Photometric light curves and polarization of close-in extrasolar giant planets. *ApJ* **540**, 504 (2000).
- [12] Vidal-Madjar, A. *et al.* An extended upper atmosphere around the extrasolar planet hd209458b. *Nature* **422**, 143 (2003).
- [13] Delrez, L. *et al.* SPECULOOS: a network of robotic telescopes to hunt for terrestrial planets around the nearest ultracool dwarfs. In *Society of Photo-Optical Instrumentation Engineers (SPIE) Conference Series*, vol. 10700 of *Society of Photo-Optical Instrumentation Engineers (SPIE) Conference Series*, 1070011 (2018). [1806.11205](#).
- [14] Jehin, E. *et al.* The SPECULOOS Southern Observatory Begins its Hunt for Rocky Planets. *The Messenger* **174**, 2–7 (2018).
- [15] McCormac, J. *et al.* DONUTS: A Science Frame Autoguiding Algorithm with Sub-Pixel Precision, Capable of Guiding on Defocused Stars. *PASP* **125**, 548 (2013). [1304.2405](#).
- [16] Lang, D., Hogg, D. W., Mierle, K., Blanton, M. & Roweis, S. Astrometry.net: Blind Astrometric Calibration of Arbitrary Astronomical Images. *AJ* **139**, 1782–1800 (2010). [0910.2233](#).
- [17] Bradley, L. *et al.* astropy/photutils: v0.7.2. Zenodo (2019).
- [18] Newville, M., Stensitzki, T., Allen, D. B. & Ingargiola, A. LMFIT: Non-Linear Least-Square Minimization and Curve-Fitting for Python. Zenodo (2014).
- [19] Astropy Collaboration *et al.* Astropy: A community Python package for astronomy. *A&A* **558**, A33 (2013). [1307.6212](#).
- [20] Astropy Collaboration *et al.* The Astropy Project: Building an Open-science Project and Status of the v2.0 Core Package. *AJ* **156**, 123 (2018). [1801.02634](#).
- [21] Pedregosa, F. *et al.* Scikit-learn: Machine learning in Python. *Journal of Machine Learning Research* **12**, 2825–2830 (2011).

A File formatting with AIJ

The files below will need to be produced for a later uploaded to ExoFOP-TESS:

- File 1: An AstrolImageJ Photometry Measurement Table, usually with an extension of .tbl, .csv, .txt, or .xls
(Note: It is preferred that AIJ measurement tables be created with an extension of .tbl. This extension can be chosen as the default for AIJ's measurement tables by selecting Edit-Options-Input/Output... from the main AIJ toolbar, and then entering .tbl for 'File extension for tables'.)
- File 2: An AstrolImageJ Plot Configuration File, with an extension of .plotcfg.
- File 3: An AstrolImageJ Photometry Aperture File, with an extension of .apertures.
- File 4: Light Curve Plots, with an extension of .png. Note: when it is not possible to easily fit the light curves of the final set of comparison stars underneath the light curves associated with the target star, then a separate file associated only with such comparison star plots may be necessary.
- File 5: A Field Image with Apertures, with an extension of .png showing the full field-of-view along with the final selection of target(s) and comparison stars shown.
- File 6: A Plate Solved Image (i.e. containing WCS FITS keywords), with an *.fit, or preferably a *.fits, extension.
- File 7: A Seeing Profile, with an extension of .png.
- File 8: A Notes and Results Text file, with a .txt extension, is a plain text observation report (see below).

File 8 should include the following information:

- The subject line should be of the form as shown in the following example: TIC 32090583.01 (TOI-218.01) on UT2023.12.25 from Saint-Ex-1m in I+z. That is, the target name, the associated TOI number, the UT date of the beginning of the observation, the name of the observatory, and the filter used in the observation. Make sure that there is a space between 'TIC' and the TIC number.
- A short statement describing the goals of the submitted run.
- A short statement describing your interpretation of the results.
- The radius of the photometry aperture in arc-seconds (on Saint-Ex, 1 pixel is 0.34 arcseconds)
- The predicted transit center time
- An indication of any Gaia stars that are contaminating the aperture and FWHM of the target star.
- Other observation notes such as maximum and standard deviation of image shift in pixels and arc-seconds, seeing conditions, other local conditions (e.g. light wind), any detrending parameters used.

Files 1 to 5 are automatically created when the results of an AIJ analysis are saved. AIJ can also be used to generate files 6, 7 while file 8 is created with a file editor.

Each of the above files should have a file name of the form targetname pp_yyyymmdd_observatory_filter_filetype.ext, where:

- targetname-pp is the TIC ID or EPIC ID, including the planet number (pp),
- yyyymmdd is the UT date/time of the beginning of the observation,
- observatory is the name of the observatory,
- filter is the filter used,
- filetype is an abbreviated description of the type of file (see the examples below), and
- ext is the appropriate extension for the type of file.

If the target has a decimal suffix for the planet number (e.g., .01), it is important to include this suffix as part of the targetname-pp by prefixing the planet number (pp) with a '-' instead of a '. As an example, for TESS target TIC32090583.01, the target name used in each file name would be TIC32090583-01. This suffix is important because it will help distinguish this planet candidate from others in a multiple planetary system. Also, for observatory and filetype, include dashes between words if the observatory name or file type is more than one word.

An example of filetype for each of the above files can be seen in the following filename examples:

- File 1: TIC32090583-01_20181225_LCO-CTIO-1m_ip_measurements.tbl
- File 2: TIC32090583-01_20181225_LCO-CTIO-1m_ip_measurements.plotcfg
- File 3: TIC32090583-01_20181225_LCO-CTIO-1m_ip_measurements.apertures
- File 4: TIC32090583-01_20181225_LCO-CTIO-1m_ip_lightcurve.png
- File 5: TIC32090583-01_20181225_LCO-CTIO-1m_ip_field.png
- File 6: TIC32090583-01_20181225_LCO-CTIO-1m_ip_WCS.fit
- File 7: TIC32090583-01_20181225_LCO-CTIO-1m_ip_seeing-profile.png
- File 8: TIC32090583-01_20181225_LCO-CTIO-1m_ip_notes.txt